# The phase transition, hygroscopicity, and thermal expansion properties of $Yb_{2-x}Al_xMo_3O_{12}$*

Li Qiu-Jie(李求杰), Yuan Bao-He(袁保合), Song Wen-Bo(宋文博), Liang Er-Jun(梁二军)†, and Yuan Bin(袁 斌)

*School of Physical Science & Engineering and Key Laboratory of Materials Physics of Ministry of Education of China, Zhenghou University, Zhengzhou* 450052, *China*

(Received 5 June 2011; revised manuscript received 24 December 2011)

Materials with the formula $Yb_{2-x}Al_xMo_3O_{12}$ ($x$ = 0.1, 0.2, 0.3, 0.4, 0.5, 0.7, 0.9, 1.0, 1.1, 1.3, 1.5, and 1.8) were synthesized and their structures, phase transitions, and hygroscopicity investigated using X-ray powder diffraction, Raman spectroscopy, and thermal analysis. It is shown that $Yb_{2-x}Al_xMo_3O_{12}$ solid solutions crystallize in a single monoclinic phase for $1.7 \leq x \leq 2.0$ and in a single orthorhombic phase for $0.0 \leq x \leq 0.4$, and exhibit the characteristics of both monoclinic and orthorhombic structures outside these compositional ranges. The monoclinic to orthorhombic phase transition temperature of $Al_2Mo_3O_{12}$ can be reduced by partial substitution of $Al^{3+}$ by $Yb^{3+}$, and the $Yb_{2-x}Al_xMo_3O_{12}$ ($0.0 < x \leq 2.0$) materials are hydrated at room temperature and contain two kinds of water species. One of these interacts strongly with and hinders the motions of the polyhedra, while the other does not. The partial substitution of $Al^{3+}$ for $Yb^{3+}$ in $Yb_2Mo_3O_{12}$ decreases its hygroscopicity, and the linear thermal expansion coefficients after complete removal of water species are measured to be $-9.1\times10^{-6}$/K, $-5.5\times10^{-6}$/K, $5.74\times10^{-6}$/K, and $9.5\times10^{-6}$/K for $Yb_{1.8}Al_{0.2}(MoO_4)_3$, $Yb_{1.6}Al_{0.4}(MoO_4)_3$, $Yb_{0.4}Al_{1.6}(MoO_4)_3$, and $Yb_{0.2}Al_{1.8}(MoO_4)_3$, respectively.

**Keywords:** negative thermal expansion material, phase transition, hygrosopicity, Raman spectroscopy

**PACS:** 65.40.De, 61.50.Ks, 82.30.Rs, 78.30.–j **DOI:** 10.1088/1674-1056/21/4/046501

## 1. Introduction

Although most materials expand as they are heated, some compounds are found to contract with increasing temperature.[1−5] This abnormal thermal expansion behavior is called negative thermal expansion (NTE). NTE has been observed in many orthorhombic tungstates and molybdates with the general formula $A_2M_3O_{12}$, where $A$ is a trivalent cation and $M$ is either Mo or W.[6−14]

The rare earth tungstates and molybdates may crystallize either in a monoclinic or orthorhombic structure depending on the $A^{3+}$ cation size, and only the orthorhombic modifications exhibit negative thermal expansion due to transverse thermal vibrations of the $A$–O–$M$ linkages of corner-sharing $AO_6$ and $MO_4$ polyhedra.[15] The monoclinic ones have an edge-shared structure which cannot accommodate transverse thermal vibrations, and therefore do not exhibit NTE. Those with larger $A^{3+}$ cation size, such as $Y_2W_3O_{12}$, $Yb_2W_3O_{12}$, $Y_2Mo_3O_{12}$, and $Yb_2Mo_3O_{12}$, crystallize in an orthorhombic structure and are highly hygroscopic, forming a trihydrate structure at room temperature.[16−18] It was found that the presence of water species hinders not only the librational and translational motions of the polyhedra but also the stretching vibrations of the $M$–O bonds, revealing that both the low frequency and high frequency phonon modes contribute to the NTE.[12] The NTE can only be observed after complete removal of the water molecules.[13] On the other hand, this family of materials with a smaller $A^{3+}$ cation size such as $Al_2(MoO_4)_3$, $Fe_2(MoO_4)_3$, and $Cr_2(MoO_4)_3$ crystallize in a monoclinic structure (space group $P2_1/a$), and undergo a phase transition from a monoclinic to orthorhombic (space group *Pnca*) structure with increasing temperature.[11,15,19,20]

Wu *et al.*[21] reported the controllable thermal expansion and phase transition of $Yb_{2x}Cr_xMo_3O_{12}$ with the aim of studying whether the NTE could be reduced through substitution of $Yb^{3+}$ with $Cr^{3+}$. They found that $Yb_{2x}Cr_xMo_3O_{12}$ had an orthorhombic for $0.0 \leq x \leq 0.4$ and a monoclinic structure for

*Project supported by the National Natural Science Foundation of China (Grant No. 10974183).

†Corresponding author. E-mail: ejliang@zzu.edu.cn

© 2012 Chinese Physical Society and IOP Publishing Ltd

$1.7 \leq x \leq 2.0$, and partial substitution of $Yb^{3+}$ for $Cr^{3+}$ exhibited depressed monoclinic to orthorhombic phase transition. Recently, we synthesized solid solutions of $Fe_{2-x}Y_xMo_3O_{12}$ ($x$ = 0.2, 0.4, 0.5, 0.6, 0.8, 1.0, 1.2, 1.4, 1.6, and 1.8) and studied the structures, phase transitions, hygroscopicity, and thermal expansion properties of these materials.[22] It was found that $Fe_{2-x}Y_xMo_3O_{12}$ crystallized in a single monoclinic structure when $x \leq 0.4$ and in a single orthorhombic structure when $x \geq 0.5$. The monoclinic-to-orthorhombic phase-transition temperature can be effectively decreased by increasing the contents of $Y^{3+}$ so that $Fe_{1.5}Y_{0.5}Mo_3O_{12}$ is already crystallized in the orthorhombic phase at room temperature and remains in this structure until at very low temperature ($< 103$ K). However, the materials of orthorhombic $Fe_{2-x}Y_xMo_3O_{12}$ with $x \geq 0.5$ are hygroscopic. In fact, how to reduce the hygroscopicity of this family of materials with larger $A^{3+}$ cations and how to reduce the monoclinic-to-orthorhombic phase-transition temperature of these with smaller $A^{3+}$ cation sizes to below room temperature still remains a great challenge. In this paper, we synthesize materials with the formula $Yb_{2-x}Al_xMo_3O_{12}$ ($0 \leq x \leq 2$), with the aim of decreasing the monoclinic-to-orthorhombic phase-transition temperature of $Al_2Mo_3O_{12}$ and to reduce the hygroscopicity of $Yb_2Mo_3O_{12}$.

## 2. Experimental details

Polycrystalline samples of $Yb_{2-x}Al_xMo_3O_{12}$ were prepared by conventional solid-state reactions. Stoichiometric amounts of $Yb_2O_3$ (purity 99.9%), $Al_2O_3$ (purity 99.9%), and $MoO_3$ (purity 99.0%) were thoroughly mingled and ground for two hours. $Yb_{2-x}Al_xMo_3O_{12}$ ($0.0 \leq x \leq 0.4$) were prepared by heating at 1173 K for 10 h and then reground followed by sintering at 1173 K for 14 h. $Yb_{2-x}Al_xMo_3O_{12}$ ($0.5 \leq x \leq 2.0$) were prepared by one-step sintering at 1173 K for 8 h. All samples were cooled down slowly in the furnace.

X-ray diffraction (XRD) measurements were carried out with an X'Pert PRO X-ray diffractometer. A Renishaw MR-2000 Raman spectrometer with 532 nm laser wavelength excitation and a Jobin–Yvon T64000 Raman spectrometer with 514.5 nm laser wavelength excitation were used for the Raman spectroscopic studies. The temperature dependence of the Raman spectra was recorded using a TMS 94 heating/freezing stage from Linkam Scientific Instruments Ltd, with an accuracy of ±0.1 K. The differential scanning calorimetry (DSC) measurements were done on an Ulvac Sinku-Riko DSC, Model 1500M/L in the temperature range of 303 K–873 K, with heating and cooling rates of 10 K/min. The linear thermal expansion coefficients of the samples were measured with a dilatometer (LINSEIS DIL L76).

## 3. Results and discussion

Figure 1 shows the XRD patterns of $Yb_{2-x}Al_xMo_3O_{12}$ for $x$ = 0, 0.2, 0.3, 0.4, 0.7, 1.3, 1.5, 1.8, and 2, respectively. The XRD patterns reveal a $Yb_2Mo_3O_{12}$-type orthorhombic structure up to the nominal composition $Yb_{1.6}Al_{0.4}Mo_3O_{12}$ with increasing $Al^{3+}$ content, indicating that 20 mol% $Yb^{3+}$ in $Yb_2Mo_3O_{12}$ can be substituted by $Al^{3+}$. However, new peaks, such as those at 15.6° and 26.8° (as indicated by $M$ in Fig. 1) originating from the $Al_2Mo_3O_{12}$-type monoclinic phase start to appear in the XRD pattern of $Yb_{1.3}Al_{0.7}Mo_3O_{12}$ and increase with increasing $Al^{3+}$ content, while the intensities of the diffraction peaks belonging to the orthorhombic structure, such as that indicated by O in Fig. 1, decrease gradually. Only weak diffraction peaks at 18.4° of the orthorhombic phase can be observed for $Yb_{0.5}Al_{1.5}Mo_3O_{12}$. A further increase in aluminum content ($x \geq 1.7$) leads to the disappearance of the orthorhombic phase and a single monoclinic phase product $Yb_{2-x}Al_xMo_3O_{12}$ is obtained. Therefore, the solid solutions of $Yb_{2-x}Al_xMo_3O_{12}$ remain orthorhombic for $0 \leq x \leq 0.4$ and monoclinic for $1.7 \leq x \leq 2.0$. Due to the large difference in the ionic radii between $Yb^{3+}$ (0.858 Å, 1 Å=0.1 nm) and $Al^{3+}$ (0.535 Å), higher substitution amounts of $Yb^{3+}$ for $Al^{3+}$ or $Al^{3+}$ for $Yb^{3+}$ do not seem possible.

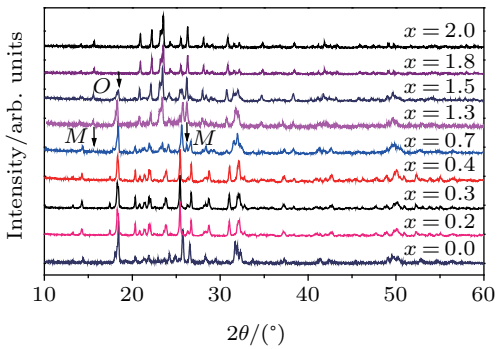



**Fig. 1.** (colour online) The X-ray diffraction patterns of $Yb_{2-x}Al_xMo_3O_{12}$ collected at room temperature.

Figure 2 shows the Raman spectra of $Yb_{2-x}Al_xMo_3O_{12}$ for $x$ = 0.0, 0.1, 0.2, 0.3, 0.4, 0.5,

0.7, 0.9, 1.1, 1.2, 1.3, 1.5, 1.8, 1.9, and 2.0, respectively. Three broad bands appear at about 950, 830, and 340 $cm^{-1}$ in the Raman spectra for $x \leq 0.4$, while additional Raman bands at about 1026 $cm^{-1}$ and 1004 $cm^{-1}$ start to appear at $x = 0.5$. Since $Yb_2Mo_3O_{12}$ has an orthorhombic structure in trihydrated form and $Al_2Mo_3O_{12}$ has a monoclinic structure at room temperature, the three broad bands at about 950, 830, and 340 $cm^{-1}$ are characteristic of the hydrated orthorhombic structure and indications of water species residing in the microchannels of $Yb_{2-x}Al_xMo_3O_{12}$.[12] However, the Raman bands at about 1026 $cm^{-1}$ and 1004 $cm^{-1}$ are characteristic of the monoclinic structure as shown by the Raman spectrum of $Al_2Mo_3O_{12}$ (see the Raman spectrum for $x = 2.0$).[23] These results suggest that the solid solutions of $Yb_{2-x}Al_xMo_3O_{12}$ remain orthorhombic for $0 \leq x \leq 0.4$, and beyond this compositional range the monoclinic phase appears. The hydrated orthorhombic features disappear completely at $x = 1.9$ and 2.0.

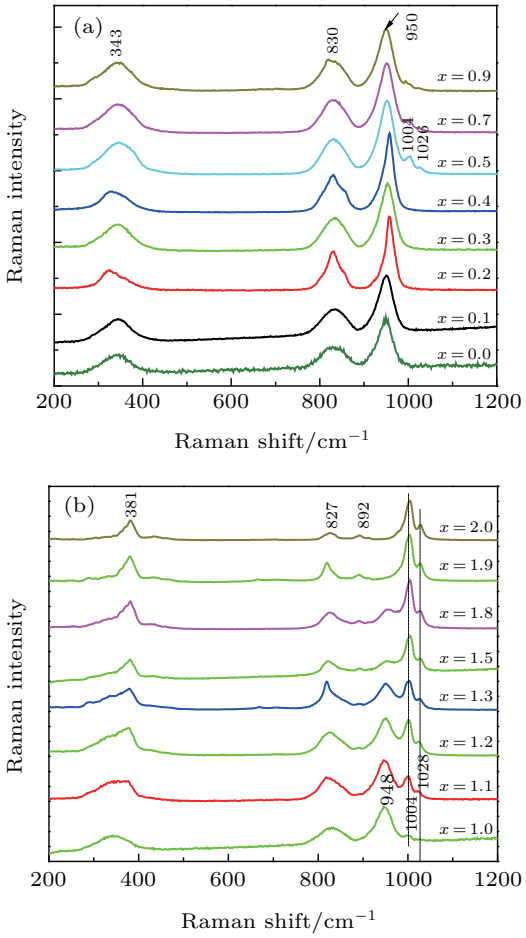



**Fig. 2.** (colour online) The Raman spectra of $Yb_{2-x}Al_xMo_3O_{12}$ measured at room temperature for $x = 0.0$, 0.1, 0.2, 0.3, 0.4, 0.5, 0.7, 0.9, 1.1, 1.2, 1.3, 1.5, 1.8, 1.9, and 2.0, respectively.

We first consider the phase transition of $Al_2Mo_3O_{12}$ by partial substitution of $Al^{3+}$ by $Yb^{3+}$. Figure 3 shows the temperature dependence of the Raman spectra of $Al_2Mo_3O_{12}$. The Raman modes between 950–1100, 750–950, and 300–450 $cm^{-1}$ can be identified as internal symmetric stretching, asymmetric stretching, and bending vibrations of the $MoO_4$ tetrahedra, respectively. With increasing temperature, the Raman band at 1028 $cm^{-1}$ becomes gradually weak and vanishes when the temperature is increased to 493 K; accompanied by splitting of the Raman band around 380 $cm^{-1}$. This indicates that $Al_2Mo_3O_{12}$ transforms from the monoclinic to orthorhombic phase between 483 K and 493 K, in accordance with the reported phase transition temperature of this material.[19,23]

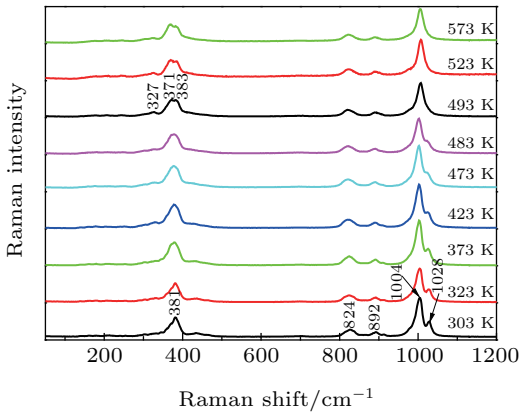



**Fig. 3.** (colour online) Temperature dependence of the Raman spectra of $Al_2Mo_3O_{12}$.

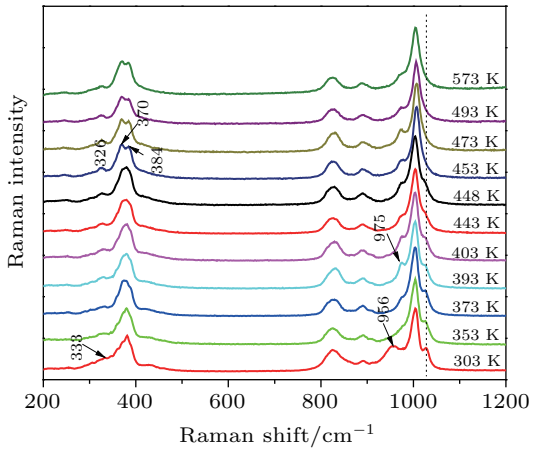



**Fig. 4.** (colour online) Temperature dependence of the Raman spectra of $Yb_{0.2}Al_{1.8}Mo_3O_{12}$.

Figure 4 shows the temperature dependence of the Raman spectra of $Yb_{0.2}Al_{1.8}Mo_3O_{12}$. It can be seen that $Yb_{0.2}Al_{1.8}Mo_3O_{12}$ is crystallized in a monoclinic structure at room temperature, as evidenced by the appearance of the Raman band at about 1027 $cm^{-1}$.

When the temperature is increased to above 453 K, this Raman band vanishes, accompanied by the splitting of the Raman band at about 380 $cm^{-1}$, suggesting that the monoclinic to orthorhombic phase transition of $Yb_{0.2}Al_{1.8}Mo_3O_{12}$ occurs at about 453 K, about 30 K lower than that of $Al_2Mo_3O_{12}$. The reduction in phase transition temperature confirms the substitution of $Yb^{3+}$ for $Al^{3+}$ and the formation of solid solution $Yb_{0.2}Al_{1.8}Mo_3O_{12}$.

Figure 5 shows the temperature dependence of the Raman spectra of $Yb_{0.5}Al_{1.5}Mo_3O_{12}$. It can be seen that the monoclinic to orthorhombic phase transition occurs at about 443 K, as indicated by the splitting of the band at about 380 $cm^{-1}$ and the vanishing of the band at 1027 $cm^{-1}$. The phase transition temperature is only about 10 K lower than that of $Yb_{0.2}Al_{1.8}Mo_3O_{12}$, demonstrating that the solubility of $Yb^{3+}$ in the solid solution $Yb_{2-x}Al_xMo_3O_{12}$ is limited ($x \geq 1.7$).

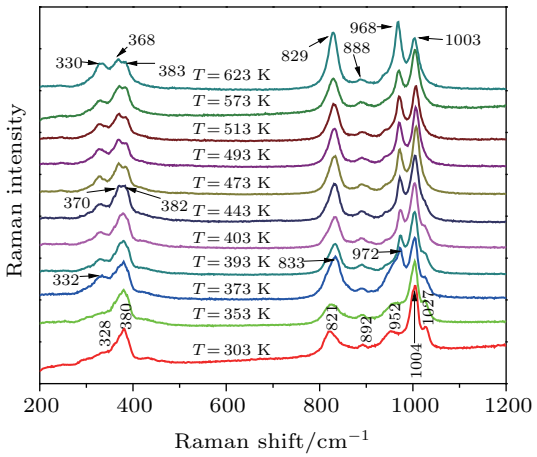



**Fig. 5.** (colour online) Temperature dependence of the Raman spectra of $Yb_{0.5}Al_{1.5}Mo_3O_{12}$.

The above results indicate that the monoclinic to orthorhombic phase transition temperature of $Al_2Mo_3O_{12}$ can be reduced by partial substitution of $Yb^{3+}$ for $Al^{3+}$ cations, though the solubility is limited. However, $Yb_{0.2}Al_{1.8}Mo_3O_{12}$ is hygroscopic as indicated by the broad band at about 956 $cm^{-1}$. It disappears above 373 K, accompanied by the appearance of a new peak at 975 $cm^{-1}$. We attribute these two bands to the Mo–O stretching vibrations in the $MoO_4$ tetrahedra connected to the $YbO_6$ octahedra since no such bands appear in $Al_2Mo_3O_{12}$. With increasing temperature, the water species will be removed, and it can be inferred that the water species interact directly with those $MoO_4$ tetrahedra connected to the $YbO_6$ octahedra, but not with those connected only to the $AlO_6$ octahedra. The phonon mode at 975 $cm^{-1}$ is suppressed by the existence of water species and activated after removal of the crystal water.

Figure 6 shows the DSC curves of $Yb_{2-x}Al_xMo_3O_{12}$ with $x$ = 2.0, 1.8, 1.5, and 1.3, respectively. It shows that the monoclinic to orthorhombic phase transition starts at about 483 K for $Al_2Mo_3O_{12}$ and at about 452 K for $Yb_{0.2}Al_{1.8}Mo_3O_{12}$, in accordance with our Raman spectral analyses shown above. The broad endothermic peak for $x$ = 1.8, 1.5, and 1.3 is related to the removal of the water species. $Al_2Mo_3O_{12}$ is not hygroscopic, but the other samples are due to the larger cation size of $Yb^{3+}$ creating microchannels in the structure.

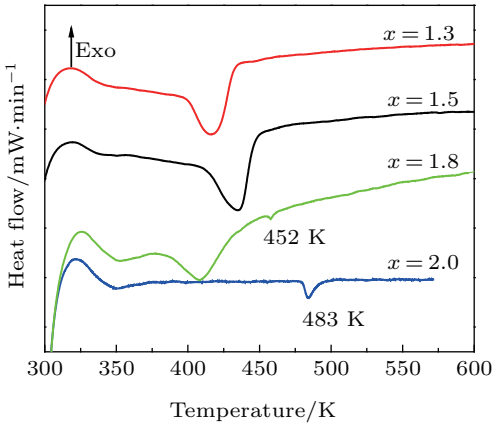



**Fig. 6.** (colour online) Typical DSC scans for $Yb_{2-x}Al_xMo_3O_{12}$ ($x$ = 2.0, 1.8, 1.5, and 1.3).

It is noticed that there is an obvious difference in the positions of the endothermic peak for $x$ = 1.8, 1.5, and 1.3. For $x$ = 1.8, the material is an edge-shared monoclinic structure which does not has large openings for the water molecules to enter. The water molecules may mainly interact with O atoms in the Yb–O–Mo linkages on the surface and hence can be released at lower temperatures. However, for $x$ = 1.5 and 1.3, the materials are composites of monoclinic and orthorhombic structures. In the corner-shared orthorhombic structure, the openings of the microchannels increase with increasing contents of $Yb^{3+}$ to allow the water molecules to enter. The water molecules in the microchannels interact with O atoms in the Yb–O–Mo and/or Al–O–Mo linkages by hydrogen bonding. Such water species may need a higher temperature to release. The smaller the microchannels are, the more difficult it is for the water species to release. Besides, due to the different polarizability in the Yb–O and Al–O bonds (electronegativity: 1.61 and 1.22 for Al and Yb) and the nonequivalent oxygen sites in the microchannels,[22] the average interaction strengths between the water species and the O atoms in the linkages may be different for $x$ = 1.5 and 1.3.

Figure 7 shows the temperature dependence of the Raman spectra of $Yb_{1.8}Al_{0.2}Mo_3O_{12}$. The bending mode shifts from 341 $cm^{-1}$ to 324 $cm^{-1}$, while the symmetric (950 $cm^{-1}$) and asymmetric (829 $cm^{-1}$) stretching modes shift to higher wavenumbers progressively with increasing temperature from 303 K to 338 K. However, sharp peaks at about 970 $cm^{-1}$ and 831 $cm^{-1}$ appear and increase successively with a further increase in temperature. The broad features disappear completely when the temperature is increased to 403 K. These changes are very similar to those of $Y_2Mo_3O_{12}$ with temperature,[12] which means that $Yb_{1.8}Al_{0.2}Mo_3O_{12}$ keeps the same structure as $Y_2Mo_3O_{12}$. At room temperature, it forms a hydrated orthorhombic structure. The changes in Raman spectra are closely correlated to the release of water species with increasing temperature. At lower temperatures, the water species without strong interactions with the polyhedra start to release, resulting in only shifts of the broad Raman bands. However, the crystal water species interacting strongly with the polyhedra in the microchannels start to release at higher temperatures, leading to the appearance of the sharp Raman bands. As in the case of trihydrate $Y_2Mo_3O_{12}$,[12] the water species hinder not only the librational and translational motions of the polyhedra, but also the internal stretching and bending vibrations.

Similar behaviors of the Raman spectral changes have been observed for $Yb_{1.7}Al_{0.3}Mo_3O_{12}$ and $Yb_{1.6}Al_{0.4}Mo_3O_{12}$ (not shown here). However, with a higher amount of substitution of $Al^{3+}$ for $Yb^{3+}$, the Raman spectra exhibit both characters of $Yb_2Mo_3O_{12}$-type orthorhombic and $Al_2Mo_3O_{12}$-type monoclinic structures, as shown in Fig. 2, for $x \geq 0.5$. This suggests that the samples synthesized for $0.5 \leq x \leq 1.7$ are composites containing both monoclinic and orthorhombic phases.

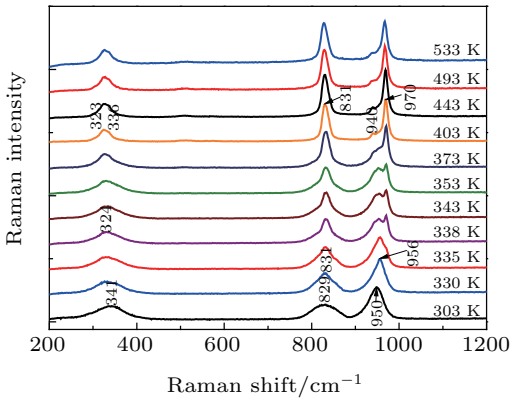



**Fig. 7.** (colour online) The temperature dependence of the Raman spectra of $Yb_{1.8}Al_{0.2}Mo_3O_{12}$.

Figure 8 shows the differential scanning calorimetry plots of $Yb_{2-x}Al_xMo_3O_{12}$ with $x = 0.1$, 0.2, 0.3, and 0.4, respectively. The DSC plots show clearly that two or three endothermic processes exist, as revealed by the different slopes corresponding to the release of different water species. The two or three processes of water release can also be seen from the TG curves, as shown by Fig. 9. The weight loss in $A_2Mo_3O_{12}$ at the first stage was attributed to the release of water species associated with the amorphous phase, and that at the second stage is related to the release of the crystal water in $A_2Mo_3O_{12}$ microchannels. From the TG curve, the number of water molecules in $Yb_{2-x}Al_xMo_3O_{12}.yH_2O$ ($x = 0.1$, 0.2, 0.3, 0.4, and 1.8) per unit formula are calculated and listed in Table 1.

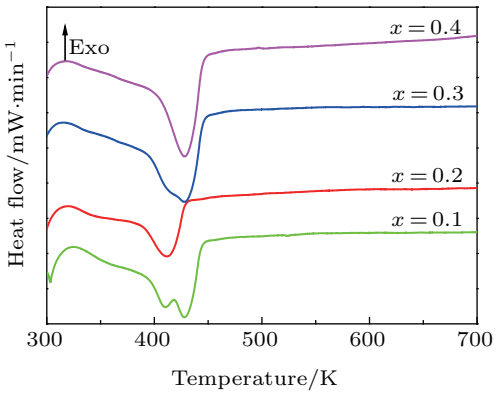



**Fig. 8.** (colour online) The typical DSC scans for $Yb_{2-x}Al_xMo_3O_{12}$ ($x = 0.1$, 0.2, 0.3, 0.4, and 0.7).

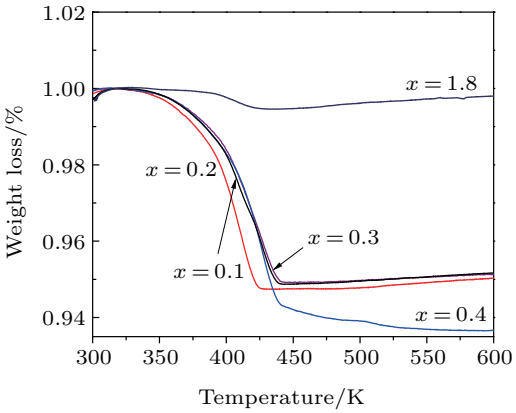



**Fig. 9.** (colour online) The TG curves of $Yb_{2-x}Al_xMo_3O_{12}$ ($x = 0.1$, 0.2, 0.3, 0.4, 1.8).

Figure 10 shows the relative length changes of $Yb_{2-x}Al_xMo_3O_{12}$ with $x = 0.2$, 0.4, 1.6, and 1.8, respectively. $Yb_{1.8}Al_{0.2}(MoO_4)_3$ and $Yb_{1.6}Al_{0.4}(MoO_4)_3$ have an orthorhombic structure and exhibit negative thermal expansion after complete removal of the crystal water species. $Yb_{0.2}Al_{1.8}(MoO_4)_3$ has a monoclinic structure and is hydroscopic at room temperature and transforms to orthorhombic at about 430 K (see Fig. 4). It shows a positive thermal expansion even after phase transition

and release of the water species. $Yb_{0.4}Al_{1.6}(MoO_4)_3$ should be dominated by monoclinic constitution with a minor orthorhombic content (see Figs. 1 and 2). It also exhibits a positive thermal expansion after phase transition and removal of water species. The linear thermal expansion coefficients after complete removal of water species are calculated using the linear parts to be $-9.1 \times 10^{-6}$/K (470 K–800 K), $-5.5 \times 10^{-6}$/K (470 K–840 K), $5.74 \times 10^{-6}$/K (430 K–1000 K), and $9.5 \times 10^{-6}$/K (430 K–950 K) for $Yb_{1.8}Al_{0.2}(MoO_4)_3$, $Yb_{1.6}Al_{0.4}(MoO_4)_3$, $Yb_{0.4}Al_{1.6}(MoO_4)_3$, and $Yb_{0.2}Al_{1.8}(MoO_4)_3$, respectively.

**Table 1.** Weight loss of $Yb_{2-x}Al_xMo_3O_{12}$ ($x = 0.1$, 0.2, 0.3, 0.4, and 1.8) and the corresponding number of crystal water molecules per unit formula.

| Sample | Weight loss | Number of water molecules | Number of crystal water |
|---|---|---|---|
| $Yb_{1.9}Al_{0.1}(MoO_4)_3$ | 5.13% | 2.44 | 1.71 |
| $Yb_{1.8}Al_{0.2}(MoO_4)_3$ | 5.25% | 2.46 | 1.59 |
| $Yb_{1.7}Al_{0.3}(MoO_4)_3$ | 5.07% | 2.32 | 1.56 |
| $Yb_{1.6}Al_{0.4}(MoO_4)_3$ | 5.69% | 2.58 | 1.52 |
| $Yb_{0.2}Al_{1.8}(MoO_4)_3$ | 0.54% | 0.17 | 0.13 |

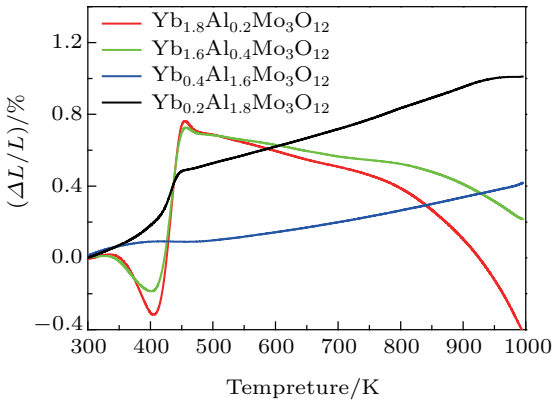



**Fig. 10.** (colour online) Relative length change with temperature of $Yb_{2-x}Al_xMo_3O_{12}$ ($x = 0.2$, 0.4, 1.6, and 1.8).

## 4. Conclusion

Materials with the formula $Yb_{2-x}Al_xMo_3O_{12}$ ($x = 0.1$, 0.2, 0.3, 0.4, 0.5, 0.7, 0.9, 1.0, 1.1, 1.3, 1.5, and 1.8) have been synthesized and their structures, phase transitions, hygroscopicities, and thermal expansion properties have been studied. It is found that $Yb_{2-x}Al_xMo_3O_{12}$ crystallizes in a single monoclinic phase for $x \geq 1.7$ and in a single orthorhombic structure for $x \leq 0.4$. The monoclinic to orthorhombic phase-transition temperature in $Al_2Mo_3O_{12}$ can be effectively decreased with partial substitution of $Yb^{3+}$ for $Al^{3+}$. The materials of the orthorhombic $Yb_{2-x}Al_xMo_3O_{12}$ with $x \leq 0.4$ are still hygroscopic, and the water species in the microchannels hindering the motions of the polyhedra still exist, but the number of water species per formula are reduced with respect to $Yb_2Mo_3O_{12}{\cdot}3H_2O$. The linear thermal expansion coefficients after complete removal of water species are measured to be $-9.1 \times 10^{-6}$/K, $-5.5 \times 10^{-6}$/K, $5.74 \times 10^{-6}$/K, and $9.5 \times 10^{-6}$/K for $Yb_{1.8}Al_{0.2}(MoO_4)_3$, $Yb_{1.6}Al_{0.4}(MoO_4)_3$, $Yb_{0.4}Al_{1.6}(MoO_4)_3$, and $Yb_{0.2}Al_{1.8}(MoO_4)_3$, respectively. This work provides some hope to reduce the monoclinic to orthorhombic phase transition temperature and to reduce the hygroscopicity of this family of materials with smaller and larger $A^{3+}$ cations by proper design.

## References


[1] Barrera G D, Bruno J A O, Barron T H K and Allan N L 2005 *J. Phys: Condens. Matter* **17** 217
[2] Mittal R and Chaplot S L 2006 *Prog. Mater. Sci.* **51** 211
[3] Grima J N, Zammit V and Gatt R 2006 *Xjenza.* **11** 17
[4] Miller W, Smith C W, Mackenzie D S and Evans K E 2009 *J. Mater. Sci.* **44** 5441
[5] Liang E J 2010 *Recent Patents Mater. Sci.* **3** 106
[6] Evans J S O , Mary T A and Sleight A W 1998 *J. Solid State Chem.* **137** 148
[7] Sleight A W 1998 *Ann. Rev. Mater. Sci.* **28** 29
[8] Marinkovic B A, Jardim P M , de Avillez R R and Rizzo F 2005 *Solid State Sci.* **7** 1377
[9] Sumithra S and Umarji A M 2006 *Solid State Sci.* **8** 1453
[10] Evans J S O, Mary T A and Sleight A W 1997 *J. Solid State Chem.* **133** 580
[11] Mary T A and Sleight A W 1999 *J. Mater. Res.* **14** 912
[12] Liang E J, Huo H L,Wang J P and Chao M J 2008 *J. Phys. Chem.* C **112** 6577
[13] Sumithra S and Umarji A M 2005 *Mater. Res. Bull.* **40** 167
[14] Liu F S, Chen X P, Xie H X, Ao W Q and Li J Q 2010 *Acta Phys. Sin.* **59** 3350 (in Chinese)
[15] Sumithra S, Tyagi A K and Umarji A M 2005 *Mater. Sci. Eng.* B **116** 14
[16] Nassau K and Levinstein H J 1965 *Phys. Chem. Solids* **36** 1805
[17] Tyagi A K , Achary S N and Mathews M D 2002 *J. Alloys Compd.* **339** 207
[18] Sleight A W and Brixner L H 1973 *J. Solid State Chem.* **7** 172
[19] Evans J S O and Mary T A 2000 *Int. J. Inorg. Mater.* **2** 143
[20] Sumithra S and Umarji A M 2004 *Solid State Sci.* **6** 1313
[21] Wu M M, Xiao X L, Hu Z B, Liu Y T and Chen D F 2009 *Solid State Sci.* **11** 325
[22] Li Z Y, Song W B and Liang E J 2011 *J. Phys. Chem.* C **115** 17806
[23] Wang Z P, Song W B, Zhao Y, Jiang Y J and Liang E J 2011 *The Journal of Light Scattering* **23** 250